Niskanen, K.; Alava, M.

Planar random networks with flexible fibers

Published in:
Physical Review Letters

DOI:
10.1103/PhysRevLett.73.3475

Published: 01/01/1994

Document Version
Publisher's PDF, also known as Version of record

Please cite the original version:
Niskanen, K., & Alava, M. (1994). Planar random networks with flexible fibers. *Physical Review Letters*, *73*(25), 3475-3478. https://doi.org/10.1103/PhysRevLett.73.3475

Planar Random Networks with Flexible Fibers

K. J. Niskanen[1] and M. J. Alava[2]

[1]*KCL Paper Science Centre, P.O. Box 70, FIN-02151 Espoo, Finland**
and U.S.D.A. Forest Service, Forest Products Laboratory, One Gifford Pinchot Drive, Madison, Wisconsin 53705-2398
[2]*Helsinki University of Technology, Laboratory of Physics, FIN-02150 Espoo, Finland*
(Received 2 May 1994; revised manuscript received 23 September 1994)

The transition in random fiber networks from two-dimensional to asymptotically three-dimensional planar structure with increasing coverage $\bar{c}$ (mean fiber length per unit area) is studied with a deposition model. Network geometry depends on the scale-free product of fiber length and $\bar{c}$ at low $\bar{c}$, and on another scale-free product of flexibility and the width-to-thickness ratio of fibers at high $\bar{c}$. The structure becomes three-dimensional or decouples from the substrate faster when fibers are stiffer. Roughness of the free surface decreases with increasing fiber flexibility.

PACS numbers: 81.15.Lm, 64.60.–i, 81.30.Dz

The mechanical properties and structure of two-dimensional random systems have recently been investigated intensively by computational and theoretical methods [1,2], but experimental studies are still few in number. However, planar fibrous materials, such as polymer films, short-fiber composites, paper, and nonwovens, provide promising possibilities for experimental work [3], in addition to being technologically interesting. The fibers in such materials are usually much longer than the sheet or film is thick, and they are almost perfectly aligned in the sheet plane [4]. The structure is therefore planar, or "layered," but no well-defined layers can be separated because of the "undulations" of the fibers in the thickness direction. If coverage (i.e., the mean fiber length per unit area) $\bar{c}$ is low, the network is almost two dimensional, and its properties must be governed by $\bar{c}$. At high $\bar{c}$ the three-dimensional "bulk" density replaces $\bar{c}$. However, e.g., mechanical properties are in both cases governed by the average number of connections (interfiber bonds) per unit fiber length or "coordination number" $\bar{n}$ [5]. Since the network is planar, we expect that its mechanical properties are independent of $\bar{c}$ if compared at a fixed $\bar{n}$.

The statistical geometry of strictly two-dimensional random fiber networks is well understood [6], but analytical models [7,8] for fiber networks with finite thickness have so far not dealt accurately with the fact that the bonding of fibers across intervening "layers" is controlled by the random pore structure. In this Letter we employ a simple computer simulation model to study the geometry of random networks of *flexible* fibers that are deposited on a two-dimensional flat substrate [growth in (2 + 1)D]. We concentrate on the coverage-driven transition from 2D to 3D network geometry with increasing coverage and show that surface roughness [9] depends on fiber stiffness. The simulation model allows the comparison of future experiments with theoretical or numerical studies [10,11,12].

We start with a two-dimensional square lattice of linear size $L = 10, \ldots, 1000$. Periodic boundary conditions are applied, except in the percolation study. The size L affects properties only close to the percolation threshold and, for surface roughness, at very high coverages. The fibers are initially straight beams of unit width and thickness, $w_f = t_f = 1$, and emphasis is given to high fiber lengths $l_f \gg 1$ [13]. Fibers are positioned and aligned in the two principal directions at random [14] in such a way that the local coverage c (number of fibers covering the cell) is always an integer. The discretization should not, of course, affect generic properties.

A "bending flexibility" T_f gives the largest allowed vertical deflection of the fibers from one lattice cell to the next (cf. Fig. 1). A high T_f gives a dense network, a low T_f a sparse one. For example, the so-called wet fiber flexibility (WFF) [15] of paper-making fibers is related to T_f through $T_f = [Cw_f(\mathrm{WFF})]^{1/4}$, where C depends on experimental details. Measured values of the wet fiber flexibility [16] and known dimensions of paper-making fibers yield $w_f T_f / t_f \geq 1$. In the simulations fibers are placed down independently, one after another, as if they were sedimenting from a dilute suspension. Each fiber is kept straight and parallel to the substrate until the first contact is made with the underlying network. Thereafter the fiber is deformed so as to lie as low as possible—not below the substrate—still obeying the deflection constraint T_f. The finite width of real fibers implies that they tend to follow a staircase pattern like that given by the model (cf. Fig. 1). The cumulative buildup of the network is a more serious departure from reality as it does not distinguish between densification mechanisms

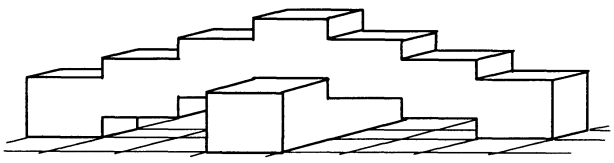

FIG. 1. Two crossing fibers on the square lattice. The height of the "steps" is $= T_f = 1/3$.

0031-9007/94/73(25)/3475(4)$06.00

such as hydrodynamic drag forces and the pressing of a filtrated fiber mat. The construction results in different top and bottom surfaces, but only the free top surface is studied here.

At low mean coverage $\bar{c}$ the in-plane properties of a planar network should be controlled by $\bar{c}/\bar{c}_c$, where $\bar{c}_c$ is the percolation threshold [17,18]. We determined $\bar{c}_c$ numerically using the following rules: (1) the network is connected when there exists a cluster of fibers that is connected to at least one cell on two opposite boundaries of the system; (2) two cells are connected by a fiber if the fiber covers them both; and (3) two fibers covering a cell are connected if the top surface of the lower fiber is in contact with the bottom surface of the upper fiber. In the case of zero fiber width, infinite flexibility (or zero fiber thickness), and continuous spatial symmetry, the percolation density is [19] $\bar{c}_c = 5.71/l_f$. This should also hold in our case despite the discrete orientations of fibers due to the excluded area principle [20,21]. Indeed, the computed threshold (cf. Fig. 2) is $\bar{c}_c \approx 5.7/l_f$ when the fibers are long and flexible ($l_f \geq 30-40$). The results in Fig. 2 are independent of L at least for $L \leq 800$.

When the fibers are short, the nonzero width w_f lowers the percolation threshold at high T_f; we find $\bar{c}_c \approx 4/l_f$ for $l_f = 7$ and $T_f > 1$, and $\bar{c}_c \approx 3.5/l_f$ for $l_f = 3$ and $T_f \geq 5$. A random walk argument suggests that in the opposite limit of $T_f \to 0$ the radius r of a cluster with N fibers is $r \sim l_f\sqrt{N}$ and therefore the thickness of a percolating cluster is $\sim t_f(L/l_f)^2 \gg L$. Thus the network becomes three dimensional, and $\bar{c}_c$ no longer characterizes its structure appropriately. Since the maximum vertical deflection per unit length of a fiber is T_f, crossover between flexible and stiff fiber behavior should occur at $T_f \sim t_f/l_f$; our data suggest $T_f \approx 4t_f/l_f$ with $t_f = 1$.

When coverage increases beyond the percolation threshold, the number of bonds per fiber and, likewise, the mechanical rigidity of the network increase [17,18]. We define the coordination number $\bar{n}$ as the average bonded surface area of a fiber, divided by $2l_f w_f$ [5]. Figure 3(a) shows how $\bar{n}$ first increases with $\bar{c}$ and then becomes asymptotically constant. Obviously the latter

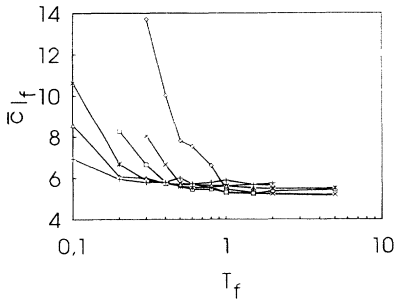

FIG. 2. The percolation threshold $\bar{c}_c$ multiplied with the fiber length l_f against T_f for fiber lengths $l_f = 3$ (◊), 5 (×), 7 (□), 11 (∗), 15 (△), and 21 (+); system size $L = 100$.

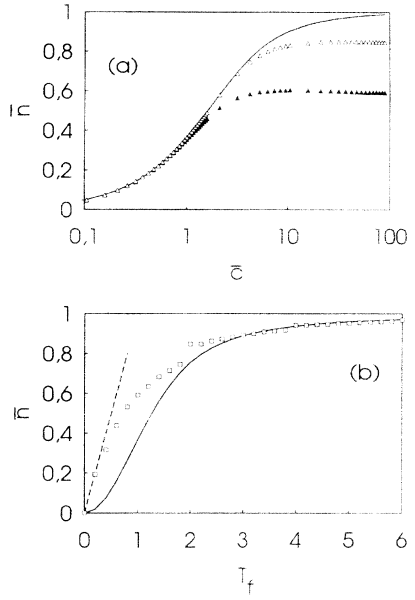

FIG. 3. Coordination number $\bar{n}$ against coverage $\bar{c}$ (a); and against fiber flexibility T_f for $\bar{c} \to \infty$ (b). In (a) $T_f = 1$ and 2 (filled and open symbols, respectively) and solid line gives Eq. (1). In (b) solid line corresponds to Eq. (2) and dashed line to $\bar{n} = T_f$. System size $L = 1000$, fiber length $l_f = 21$.

happens when the substrate has no effect on $\bar{n}$ anymore. The network has then become three dimensional, and every new layer has the same structure as the preceding one. However, in the case of $T_f \to \infty$ this never happens, and the coordination number is that of a two-dimensional network at all coverages, given by [6]

$$\bar{n} = 1 - [1 - \exp(-\bar{c})]/\bar{c} \qquad (1)$$

[cf. Fig. 3(a)]. The crossover from 2D to 3D can be roughly located by observing that at low coverages there are relatively few pores *inside* the network. Thus height differences between neighboring cells are of the order $\sim\sqrt{\bar{c}}/w_f$ since coverage is Poisson distributed [6]. Pores start to develop inside the network when $T_f/t_f \sim \sqrt{\bar{c}}/w_f$. Equation (1) then yields

$$\bar{n} = 1 - \{1 - \exp[-(T_f w_f/t_f)^2]\}/(T_f w_f/t_f)^2 \qquad (2)$$

for the asymptotic 3D structure. The computed values agree reasonably with Eq. (2) for large T_f as Fig. 3(b) shows (for $w_f = t_f = 1$). For $T_f \ll 1$ we can estimate that on the average each fiber (with $l_f \gg w_f$) on the surface of the network prevents new fibers from making contact with others on $l_f t_f/T_f$ sites, while bonding with the fiber in question is possible in $w_f l_f$ cells. Hence $\bar{n} = w_f l_f/(w_f l_f + l_f t_f/T_f) \approx (T_f w_f/t_f)$ at high coverages [dashed line in Fig. 3(b)]. The simulation results in Fig. 3 were found to be independent of the fiber length at least for $l_f \geq 5$. The reproducible discontinuities at $T_f = 2$ and 4 in Fig. 3(b) are artifacts of the discrete model.

In contrast to $\bar{n}$, the three-dimensional bulk density ρ *decreases* with increasing coverage (provided that surfaces pores are excluded), since at low coverage there are initially no pores inside the sheet. In reality thickness measurements have finite spatial resolution, and usually they underestimate the true density. A "coarse-grained" or "apparent" density was calculated from the model to mimic real measurements. The results were similar to the $n(\bar{c})$ curves in Fig. 3(a). At high coverages (thicknesses) even an apparent density is independent of surface roughness and equal to the "true" density. Since the coordination number is tedious to measure directly, the 3D bulk density is sometimes used to estimate it. Our results (Fig. 4) indicate that if $\bar{c}$ is held constant and T_f is varied, then $\bar{n}$ is indeed roughly proportional to ρ. This also holds for apparent densities. However, if T_f is held constant and coverage is increased, the true 3D density decreases and hence cannot be proportional to $\bar{n}$ (cf. discussion above), but an apparent density may still be.

As the local coverage is Poisson distributed [6], the standard deviation of local coverage is $\sigma_c = \sqrt{\bar{c}}$. This holds very well in our simulations. The flat substrate affects the network structure at small $\bar{c}$, but as $\bar{c}$ grows the structure of new layers becomes stable, independent of $\bar{c}$. Then, for example, the standard deviation of the number of pores per cell (p) becomes $\sigma_p \to P(T_f)\sqrt{\bar{c}}$. The amplitude $P(T_f)$ decreases with increasing T_f. Areas of high coverage have few pores, and therefore $P < 1$. The average number of pores is directly related to the coordination number through

$$\bar{n} = 1 - \frac{p+1}{\bar{c}}[1 - \exp(-\bar{c})] \qquad (3)$$

which follows as a generalization of Eq. (1).

The roughness σ_t of the free surface can be defined as the standard deviation of the local surface height t, the distance between the free surface and substrate. Through trial and error we found that the simulation results can be expressed as

$$\sigma_t^2 \approx \bar{c} t_f^2 [A(w_f T_f / t_f) + B(\bar{c})] \qquad (4)$$

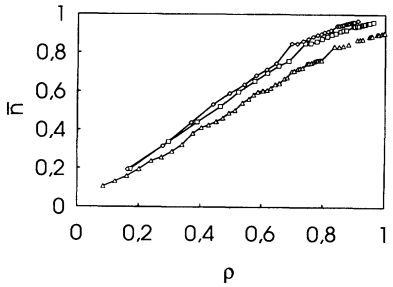

FIG. 4. Coordination number $\bar{n}$ against density ρ when fiber flexibility T_f varies. Coverage $\bar{c} = 10.5$ (△), 31.5 (□), and 94.5 (◊). Fiber length $l_f = 21$, system size $L = 1000$.

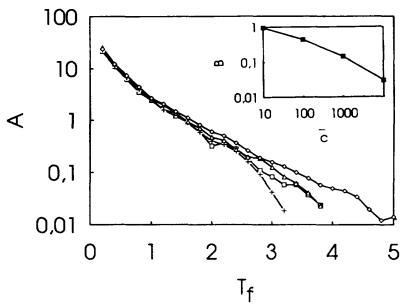

FIG. 5. Function $A(T_f)$, Eq. (1), for coverages $\bar{c} = 10$ (□), 100 (+), 10^3 (△), and 10^4 (◊). Fiber length $l_f = 5$, system size $L = 100$. Inset shows function $B(\bar{c})$ on log-log scale.

(of course, we have data only for $t_f = w_f = 1$). The functions A and B are shown in Fig. 5 for system size $L = 100$, $T_f \leq 5$, and $\bar{c} \leq 10^4$. They are independent of fiber length as long as $l_f \geq 5$. It was easy to decompose σ_t into A and B since at large T_f, σ_t turned out to be a function of $\bar{c}$ only (or $A \to 0$). The prefactor $\bar{c}$ in Eq. (4) is motivated by the Poissonian deposition process. As coverage increases, B becomes smaller and eventually σ_t grows as $\sim\sigma_c = \sqrt{\bar{c}}$. This corresponds to a decoupling of the surface from the flat substrate. The decoupling is fast with stiff fibers (A large), since stiff fibers cannot "feel" the substrate from high above. For the same reason the case of stiff fibers seems to correspond to a *low* surface tension in ordinary growth models [9] as no long range correlations occur in the surface height. Indeed, making T_f small gives a rough surface. In fact, our model is similar to the Vold model [9,22]. Details of the growth behavior at high coverage, including the effects of system size, are beyond the scope of this study and will be presented elsewhere.

Summarizing, we have presented a computer simulation study of planar random fiber networks. The model provides a connection between the properties of real planar fiber networks and ideal two-dimensional networks. The results can be represented in closed form only in a few cases, but the model is simple enough so that the numerical solution can be easily used, e.g., in the analysis of experimental results.

This study was financially supported by the Technology Development Centre of Finland and by the Academy of Finland which is gratefully acknowledged.

*Present and permanent address.

[1] *Statistical Models for the Fracture of Disordered Media*, edited by H. J. Herrmann and S. Roux (North-Holland, Amsterdam, 1990).
[2] M. Sahimi, Physica (Amsterdam) **186A**, 160 (1992).
[3] J. Kertesz, Physica (Amsterdam) **191A**, 208 (1992).

[4] B. Radvan, in *The Fundamental Properties of Paper Related to its Uses*, edited by F. Bolam (British Paper and Board Ind. Fed., London, 1976), pp. 137–147.
[5] For paper the quantity corresponding to the coordination number is the relative bonded area (RBA) of the fibers. See O. J. Kallmes, H. Corte, and G. Bernier, Tappi J. **46**, 502 (1963).
[6] H. Corte and O. J. Kallmes, Tappi J. **43**, 737 (1960).
[7] O. J. Kallmes, H. Corte, and G. Bernier, Tappi J. **44**, 519 (1961).
[8] J. Görres, C. S. Sinclair, and A. Tallentire, Paperi ja Puu **71**, 54 (1989); J. Gorres and P. Luner, J. Pulp Paper Sci. **18**, J127 (1992).
[9] J. Krug and H. Spohn, in *Solids Far from Equilibrium: Growth, Morphology, Defects*, edited by C. Godréche (Cambridge Univ. Press, Cambridge, 1991), pp. 479–582.
[10] M. J. Alava and R. K. Ritala, J. Phys. Condens. Matter **2**, 6093 (1990); M. J. Alava and R. K. Ritala, Phys. Scr. **T33**, 155 (1990).
[11] J. A. Åström and K. J. Niskanen, Europhys. Lett. **21**, 557 (1993).
[12] J. Åström, S. Saarinen, K. Niskanen, and J. Kurkijärvi, J. Appl. Phys. **75**, 2383 (1994).
[13] Fiber thickness is arbitrary in our study. For papermaking fibers $l_f/t_f \geq l_f/w_f \simeq 20$–$50$.
[14] We use the R250 random number generator: S. Kirkpatrick and E. Stoll, J. Comput. Phys. **40**, 517 (1981).
[15] R. Steadman and P. Luner, in *Papermaking Raw Materials*, edited by V. Punton (Mechanical Engineering Publ. Ltd., London, 1985), pp. 311–338.
[16] L. Paavilainen, Paperi ja Puu **46**, 689 (1993).
[17] S. Kirkpatrick, Rev. Mod. Phys. **45**, 574 (1973).
[18] L. M. Schwartz, S. Feng, M. F. Thorpe, and P. N. Sen, Phys. Rev. **32**, 4607 (1985).
[19] G. E. Pike and C. H. Seager, Phys. Rev. B **10**, 1421 (1974).
[20] I. Balberg, Phys. Rev. B **31**, 4053 (1985).
[21] K. Tobochnik, M. A. Dubson, M. L. Wilson, and M. F. Thorpe, Phys. Rev. A **40**, 5370 (1989).
[22] M. J. Vold, J. Colloid Sci. **14**, 168 (1959).